

**Smectic phase in a system of hard ellipsoids with isotropic attractive interactions**

Elvira Martín del Río\* and Enrique de Miguel†

*Department of Chemical Engineering, Imperial College London, South Kensington Campus, London SW7 2AZ, United Kingdom*

(Received 21 January 2005; published 11 May 2005)

The smectic phase is studied for a thermotropic fluid model consisting of aligned hard ellipsoids with superimposed square-well attractive interactions of variable range. The system is analyzed using a density functional theory in which the hard-core contributions to the free-energy functional are treated within a nonlocal weighted density approximation and the attractive contributions are considered at a mean-field level. In the absence of attractions the model reduces, under appropriate scaling, to a fluid of hard spheres and therefore does not exhibit smectic ordering. It is shown that above a certain value of the square-well range, smectic ordering is stable relative to the nematic state at densities well inside the fluid region. The nematic–smectic-*A* transition is found to be continuous at high temperatures and first order at low temperatures, these two regimes being separated by a tricritical point at an intermediate temperature. These predictions have been confirmed by computer simulation of the model fluid. The results highlight that smectic ordering can be stabilized by coupling anisotropic short-range repulsions with the isotropic contribution of the soft attractive interactions. By increasing the pressure, the range of stability of the smectic phase is seen to decrease. At sufficiently high pressure, the smectic phase is suppressed, and the solid phase dominates. Our calculations show that smectic ordering is no longer stable if the range of the attractions is made too long ranged.

DOI: 10.1103/PhysRevE.71.051710

PACS number(s): 64.70.Md, 61.30.Cz, 05.70.Fh

**I. INTRODUCTION**

The main goal of any molecular theory of liquid crystals is the prediction of phase behavior and phase transitions from the interactions at a molecular level [1]. These interactions, however, are either not known exactly or expected to be quite complicated, due to the complexity of the molecular structure of typical liquid crystal forming molecules [2]. Interactions in simple liquids, though still complex, can be understood in terms of short-range repulsions and longer ranged dispersion attractions. Modeling the repulsive interactions by hard spheres and considering the attractions as a perturbation treated at a mean-field level is at the heart of van der Waals–like theories of simple (isotropic) fluids [3]. Whether this approach also applies to the description of mesophases is far from being trivial, but it provides a reasonable starting point and, certainly, has guided many molecular theories of liquid crystals.

Here, we will be concerned with the description of the thermotropic smectic-*A* phase, focusing on the importance of the coupling between the anisotropic short-range repulsions and the soft attractive interactions in stabilizing smectic ordering in a particular molecular model.

In the smectic-*A* phase, the molecules are preferentially aligned along one direction (as in a nematic liquid crystal) and in addition form layers perpendicular to this direction

[4]. One of the earliest molecular theories for smectics was developed by McMillan [5] and Kobayashi [6]. This mean-field theory can be regarded as an extension of Maier-Saupe’s approach of nematics to include the possibility of translational order. Depending on the model parameters and temperature, smectic ordering is stabilized through the soft anisotropic attractive interactions, the steric effects playing a negligible role in stabilizing the phase. The McMillan-Kobayashi (MK) theory has been further refined [7–11] (see also Ref. [1] for a review on the subject), but the basic structure of the theory remains the same (see, however, Ref. [11]). Despite its relative success, the MK theory suffers from a number of limitations, the most severe being that excluded-volume interactions arising at short distances due to steric effects are fully neglected. Considering that the nematic-to-smectic transition can be loosely viewed as a one-dimensional crystallization, it is difficult to think of the short-range packing interactions of the hard molecular cores as a side effect in bringing about smectic ordering [12].

This issue is at the heart of theories which rely (directly or indirectly) on Onsager’s ideas [13] that (nematic) orientational ordering can be understood as a result of the anisotropic excluded-volume interactions without having to invoke attractive interactions. The fact that purely repulsive interactions can stabilize smectic order has been widely demonstrated by computer simulations on a number of hard-particle systems [14–18]. Simulation has also highlighted the importance of the anisotropy associated to the molecular shape: a system of hard spherocylinders, for instance, can develop smectic order, whereas a system of hard ellipsoids does not seem likely to stabilize the smectic phase. The application of Onsager’s theory to the description of smectic ordering is severely limited: at densities at which the smectic phase is expected, the validity of the truncation of the virial series at the level of the second virial coefficient is questionable in the case of very long rods and unreliable for most

\*Permanent address: Departamento de Ingeniería Eléctrica y Térmica, Escuela Politécnica Superior de La Rábida, Universidad de Huelva, 21819 Huelva, Spain.

†Author to whom correspondence should be addressed. Permanent address: Departamento de Física Aplicada, Facultad de Ciencias Experimentales, Universidad de Huelva, 21071 Huelva, Spain. Email address: demiguel@uhu.es

typical molecular elongations in liquid crystals [19].

Although attempts have been made to incorporate higher-order terms in the virial expansion of the free energy [20,21] a more promising route for the description of hard-core effects in smectics is provided by density functional approximations for the free energy [22–31]. These theories can be formulated in a variety of ways (see Ref. [1] for a review). A widely used approach relies on the theory of the inhomogeneous hard-sphere fluid [32] to account for the nonuniform density distribution of the smectic phase. The nonlocal structure of the smectic phase is described in terms of a coarse-grained density, which is obtained from a weighting procedure. The latter is not unique and different schemes (weighted-density [11,23–27], smoothed-density [28–30], modified weighted-density [31] approximations) have been devised. The theoretical predictions are, in most cases, in qualitative agreement with results from computer simulation [17]. One may conclude that the density functional formalism provides a consistent approach to understand the role of the short-range hard-core effects in forming the smectic phase.

A proper treatment of smectic order in thermotropic liquid crystals, however, must go beyond hard-body models and include explicitly both repulsive and attractive interactions. A suitable framework is provided by a generalization of van der Waals-like theories to systems of nonspherical particles. This approach was first developed by Gelbart and Baron [33] and has been used with reasonable success to study the nematic phase [34–39]. According to Gelbart and Baron [33], the pair interaction energy can be written as the sum of a repulsive term (arising from the anisotropic hard cores) and an attractive term. The latter is given by a truncated expansion in spherical harmonics with distance-dependent coefficients. In the spirit of van der Waals theories the free energy of the system consists of two contributions: one arising from the hard cores, and a second one that includes the attractive interactions at a mean-field level. As the mean-field average is restricted to those configurations allowed by the (impenetrable) cores, these two terms are highly correlated. As a consequence, the hard-rod repulsions build in anisotropic correlations in the attractive contribution even if the attractive interactions have spherical symmetry. Moreover, it has been noticed [34,37] that for nematics, the main contribution to the attractive term in the free energy comes from the lowest-order (isotropic) term of the attractive interactions (modulated by the anisotropic hard core) and not from the higher-order (angular dependent) terms.

The primary purpose of our current work is to show that smectic ordering can be stabilized by the coupling between the anisotropic short-range repulsions and the *isotropic* contribution of the attractive interactions. We assume a specific molecular model in which the hard core is represented by a hard ellipsoid and the soft attractive interactions are given by an spherically symmetric square well. We further simplify the molecular model by neglecting orientational fluctuations.

A related study was performed by Kloczkowski and Stecki [40] for a system of hard spherocylinders interacting with an isotropic  $r^{-6}$  attractive energy. The results, however, have to be taken with some care as it was concluded (erroneously, as was later pointed out [14]) that smectic ordering

in a system of hard spherocylinders could only be stabilized by the attractive interactions; the fact that no smectic phase could be stabilized in the absence of attractive interactions is probably related to the drastic low-density Onsager approximation used to account for the hard core effects. Nakagawa and Akahane [41] considered a similar molecular model (hard spherocylinder plus attractive tail) but now including an extra angular-dependent term with the same symmetry as that used by McMillan. The repulsive contribution is again treated under the Onsager approximation and the attractive contribution at a mean-field level. The attractions, however, are averaged over a spherically symmetric region (using a cutoff that depends on the molecular size). This certainly simplifies the calculations but neglects the anisotropic shape of the molecule. A related approach, although not based on a well-defined molecular model, has been given by Mederos and Sullivan [11]. Hard-core effects are modeled by parallel hard ellipsoids and the attractive interaction includes an additional term coupling the intermolecular vector and the molecular orientations. The main innovation introduced by Mederos and Sullivan is that the contribution to the free energy arising from the short-range repulsions is consistently described by using a nonlocal density functional for the free energy. Smectic ordering appears as a consequence of the (anisotropic) attractive interactions, although the hard-core interactions turn out to be crucial in determining the smectic wavelength, which is calculated in a self-consistent way. The approach of Mederos and Sullivan [11], as well as that of Nakagawa and Akahane [41], can be regarded as generalized versions of the McMillan-Kobayashi theory but with explicit consideration of steric effects. Anisotropic correlations originated from the hard core are neglected and the anisotropic attractive interactions are the driving force for smectic ordering.

Here, we consider a slightly different approach and investigate the importance of the anisotropy induced by the hard cores into the attractive pair potential as an effective mechanism for the onset of smectic ordering. In order to clarify this point, the molecular model has been intentionally chosen so that the hard-core interactions by themselves do not stabilize smectic order. The attractive interactions contain no *explicit* anisotropic, angular-dependent contribution. An additional purpose of this work is to provide an insight on the role of the range of the attractive interactions in bringing about smectic ordering.

The paper has been organized as follows. A brief account of the molecular model used in the present work is given in Sec. II. Section III treats the nonlocal density functional theory used throughout this work. Our treatment of the repulsive contributions to the free energy functional rests heavily in that first introduced by Mederos and Sullivan [11]; differences are to be found, however, in the way the attractive contributions are considered. Details are also given on the bifurcation analysis used to the study of the stability of the smectic phase relative to the nematic and on the calculation of the tricritical point. Section IV includes the results for a fixed molecular elongation and a number of values of the range of the attractive interactions. We summarize our main conclusions in Sec. V.

## II. MOLECULAR MODEL

We consider a fluid system of  $N$  axially symmetric particles. Orientational fluctuations are disallowed by constraining the molecular long axis to remain parallel to a common direction, here taken as the  $z$  axis. The interaction energy between a pair of molecules is expressed as

$$u(\mathbf{r}) = u_{\text{rep}}(\mathbf{r}) + u_{\text{att}}(\mathbf{r}), \quad (1)$$

where  $u_{\text{rep}}$  and  $u_{\text{att}}$  represent the repulsive and attractive interaction energy, respectively, and  $\mathbf{r}$  is the intermolecular vector. The molecules are assumed to consist of a hard core with ellipsoidal shape determined by its long ( $L$ ) and short ( $D$ ) principal axes. A measure of the molecular anisotropy is given by  $\kappa=L/D$ . The repulsive interaction is then given by

$$u_{\text{rep}}(\mathbf{r}) = \begin{cases} \infty & \text{if } r \leq \sigma(\hat{\mathbf{r}}), \\ 0 & \text{if } r > \sigma(\hat{\mathbf{r}}), \end{cases} \quad (2)$$

where  $\sigma(\hat{\mathbf{r}})$  is the distance of closest approach between two parallel hard ellipsoids (PHE). Here,  $r$  is the distance between the molecular centers of mass, and  $\hat{\mathbf{r}}=\mathbf{r}/r$  is a unit vector along the intermolecular vector. As regards the attractions, these are typically incorporated through a truncated expansion of the attractive potential in spherical harmonics with  $r$ -dependent coefficients. The resulting anisotropic potential is then fully defined by a judicious choice of the distance dependence of the expansion coefficients. Instead, the soft attractions will be modeled here by a square-well interaction:

$$u_{\text{att}}(\mathbf{r}) = \begin{cases} -\epsilon & \text{if } \sigma(\hat{\mathbf{r}}) < r < \lambda, \\ 0 & \text{if } r \geq \lambda, \end{cases} \quad (3)$$

where  $\lambda$  is the range and  $\epsilon$  the strength of the attractive interactions. According to Eq. (3), the attractive pair interaction *outside the hard core* is spherically symmetric and contains no explicit anisotropic terms.

Evans *et al.* [42] introduced a similar model consisting of an arbitrary hard nonspherical core embedded in a spherical square well. The model, without the constraint of perfectly molecular alignment, has been applied to the study of nematic liquid crystals with the hard core taken to be either an ellipsoid or a spherocylinder [43–51]. In most cases (see, however, Ref. [51]) the range  $\lambda$  of the attractive interactions was taken to be  $\lambda/D \geq \kappa$  (note that  $\kappa=L/D$  for ellipsoids and  $\kappa=L/D+1$  for spherocylinders). For highly anisotropic molecules, this choice may give rise to an overestimation of the range of the attractions. In this work, different choices of  $\lambda$  will be considered with the restriction  $\lambda/D < \kappa$ .

## III. THEORY

### A. Free energy

We consider a fluid system of  $N$  molecules interacting through the pair potential defined in Eqs. (1)–(3). The system is enclosed in a volume  $V$  at a temperature  $T$ .

In keeping with the density-functional formalism for non-uniform fluids, the system is characterized by the one-particle distribution function  $\rho(\mathbf{r})$ , which gives the local

density of particles at position  $\mathbf{r}$ . The structure and thermodynamics of the system at equilibrium follow from minimization of the free-energy functional with respect to  $\rho(\mathbf{r})$ . The free-energy functional can be expressed as a sum of two terms,

$$F[\rho(\mathbf{r})] = F_{\text{rep}}[\rho(\mathbf{r})] + \frac{1}{2} \int d\mathbf{r} d\mathbf{r}' \rho(\mathbf{r}) \rho(\mathbf{r}') u_{\text{att}}(|\mathbf{r} - \mathbf{r}'|), \quad (4)$$

where  $F_{\text{rep}}$  includes the contributions to the free energy coming from the repulsive interactions. The last term in Eq. (4) includes the contribution from the attractive interactions and is treated here at a mean-field level.

The repulsive term can be expressed as

$$F_{\text{rep}}[\rho(\mathbf{r})] = k_B T \int d\mathbf{r} \rho(\mathbf{r}) \{ \ln[\Lambda^3 \rho(\mathbf{r})] - 1 \} + \Delta F_{\text{rep}}[\rho(\mathbf{r})], \quad (5)$$

where  $k_B$  is Boltzmann's constant and  $\Lambda$  is the thermal de Broglie wavelength. In the above expression, the first term is the contribution from the ideal gas, and  $\Delta F_{\text{rep}}$  is the excess part, which contains all the contributions from the hard-core interactions. The latter term is treated within a nonlocal approximation [32], i.e.,

$$\Delta F_{\text{rep}}[\rho(\mathbf{r})] = \int d\mathbf{r} \rho(\mathbf{r}) \Delta \psi_{\text{PHE}}(\bar{\rho}(\mathbf{r})), \quad (6)$$

where  $\Delta \psi_{\text{PHE}}$  is the (excess) free energy per particle of a homogeneous system of parallel hard ellipsoids (PHE). Expression (6) has a form resembling the local-density approximation (see, for instance, Ref. [32]) although the free energy is evaluated at a coarse-grained density  $\bar{\rho}$  that takes into account the nonlocal structure of the fluid. There is no unique way to define  $\bar{\rho}$  in terms of  $\rho(\mathbf{r})$ . Here we follow the weighted-density approximation (WDA) developed by Tarazona [32] for the inhomogeneous hard-sphere (HS) system, which assumes that the smoothed density is given by an average of  $\rho_{\text{HS}}(\mathbf{r})$  weighted by a suitable function  $w$  that depends on  $\bar{\rho}_{\text{HS}}$ :

$$\bar{\rho}_{\text{HS}}(\mathbf{r}) = \int d\mathbf{r}' \rho_{\text{HS}}(\mathbf{r}') w(|\mathbf{r} - \mathbf{r}'|; \bar{\rho}_{\text{HS}}(\mathbf{r})). \quad (7)$$

The explicit expression of the weight function can be found elsewhere (see, for instance, Ref. [11]). The corresponding smoothed  $\bar{\rho}$  for a system of PHE molecules can be simply obtained from that of the HS system by considering the anisotropic transformation that maps ellipsoids into spheres [52]:

$$\bar{\rho}_{\text{PHE}}(\mathbf{r}) \equiv \bar{\rho}(\mathbf{r}) = \frac{1}{\kappa} \bar{\rho}_{\text{HS}}(\mathbf{A} \cdot \mathbf{r}). \quad (8)$$

Here,  $\mathbf{A}$  is the diagonal tensor [with components 1, 1,  $(\kappa)^{-1}$ ] that defines the transformation of the PHE system into a system of HS of diameter  $D$ . Recall that  $\kappa=L/D$ . Using (7) and (8) one arrives at [11]

$$\bar{\rho}(\mathbf{r}) = \int d\mathbf{r}' \rho(\mathbf{r} + \mathbf{A}^{-1}\mathbf{r}') w(|\mathbf{r}'|; \kappa \bar{\rho}(\mathbf{r})). \quad (9)$$

Finally, we use the Carnahan-Starling approximation for  $\Delta\psi_{\text{PHE}}$  in Eq. (6):

$$\Delta\psi_{\text{PHE}}(\eta) = k_B T \frac{4\eta - 3\eta^2}{(1 - \eta)^2}, \quad (10)$$

where  $\eta = \rho v_0$  is the packing fraction;  $v_0 = (\pi/6)\kappa D^3$  being the volume of the ellipsoidal molecule. Equations (5)–(10) completely determine the contribution of the repulsive interactions to the free energy.

In the following, the one-particle distribution function will be only permitted to vary along  $z$ , i.e.,  $\rho(\mathbf{r}) = \rho(z)$  thereby only allowing for the description of the nematic and smectic- $A$  phases. With this restriction, the free-energy functional cannot account for smectic phases with in-plane order or the solid phase.

We now turn to the attractive term of the free energy [second term in Eq. (4)]. After integration in the  $x$ - $y$  plane, the attractive free energy per unit volume  $f_{\text{att}}$  can be written in terms of an effective attractive potential  $\bar{u}_{\text{att}}$  as

$$\beta f_{\text{att}} = \frac{1}{2} \beta \frac{1}{d} \int_0^d dz \rho(z) \int dz' \rho(z') \bar{u}_{\text{att}}(|z - z'|). \quad (11)$$

Here,  $\beta = (k_B T)^{-1}$ ,  $d$  is the smectic period, and

$$\bar{u}_{\text{att}}(|z - z'|) = \int d\mathbf{R} u_{\text{att}}(\mathbf{R}, |z - z'|), \quad (12)$$

where we have used the notation  $\mathbf{r} - \mathbf{r}' = (\mathbf{R}, z - z')$  for the intermolecular vector. Inserting  $u_{\text{att}}$  from Eq. (3) into Eq. (12) and performing the integration, yields for  $\bar{u}_{\text{att}}$ :

$$\bar{u}_{\text{att}}(z) = \begin{cases} \bar{u}_0 + \bar{u}_2 z^2 & \text{if } |z| < z_{\text{max}}, \\ 0 & \text{if } |z| > z_{\text{max}}, \end{cases} \quad (13)$$

where

$$\bar{u}_0 = -\epsilon\pi(\lambda^2 - D^2), \quad \bar{u}_2 = \epsilon\pi(\kappa^2 - 1)/\kappa^2, \quad (14)$$

and  $z_{\text{max}} = (-\bar{u}_0/\bar{u}_2)^{1/2}$ . Recall that we are limiting ourselves to the case  $D \leq \lambda \leq L$ . We finally arrive at the following expression for the free-energy functional (per unit volume):

$$\beta f[\rho(z)] = \frac{1}{d} \int_0^d dz \rho(z) \left\{ \ln[\Lambda^3 \rho(z)] - 1 + \beta \Delta\psi_{\text{PHE}}(\bar{\rho}(z)) + \frac{1}{2} \beta \int dz' \rho(z') \bar{u}_{\text{att}}(|z - z'|) \right\}. \quad (15)$$

By functional minimization of the free energy (15), one obtains the equilibrium density  $\rho(z)$  at each input value of the temperature  $T$  and average number density  $\rho$ . For numerical convenience, we consider the following truncated Fourier expansion of the one-particle density:

$$\rho(z) = \rho \left[ 1 + \sum_{n=1}^m \rho_n \cos(nqz) \right], \quad (16)$$

where the Fourier coefficients  $\rho_n$  with  $n=1, \dots, m$  define a set of (dimensionless) translational order parameters,  $q$  is the wavevector along  $z$ , and  $d=2\pi/q$  is the wavelength of the density modulation. The nematic phase corresponds to all  $\rho_n$  equal to zero. When  $\rho(z)$  from Eq. (16) is inserted into Eq. (15), the free energy becomes a function of the wave vector and the order parameters, i.e.,  $f=f(T, \rho; q, \rho_n)$ . In practice, the equilibrium distribution  $\rho(z)$  is obtained by minimizing  $f$  with respect to the variational parameters  $d$  and the order parameters  $\rho_n$  using Powell's method [53] at given input values of the average density  $\rho$  and temperature  $T$ .

## B. Nematic-smectic transition

By construction, the free-energy functional (15) can only account for nematic and smectic- $A$  phases. The relative stability of both phases has been proved by using a bifurcation analysis [20]. For a given value of the temperature, this amounts to finding the (average) density at which the nematic phase becomes unstable relative to a phase with a density modulation along  $z$ . If the nematic-smectic- $A$  transition is continuous, the bifurcation density  $\rho^*$  fixes the location of the transition, i.e.,  $\rho_{\text{NA}} = \rho^*$ . However, as first shown by Meyer and Lubensky [54], the transition may also be first order (even for systems with saturated nematic order) due to the coupling between the translational order parameters. In this case, the bifurcation point lies on the spinodal line and the actual transition densities  $\rho_N$  and  $\rho_A$  bracket the bifurcation density, i.e.,  $\rho_N < \rho^* < \rho_A$ .

We start by expanding the free energy in powers of the order parameters around the nematic phase  $\rho_n=0$  ( $n=1, \dots, m$ ). To determine the bifurcation point and the order of the transition, it is sufficient to expand the free energy to fourth order in  $\rho_1$  and  $\rho_2$ , which yields [54]

$$\begin{aligned} f(T, \rho; q, \rho_1, \rho_2) = & f_0(T, \rho) + \frac{1}{2} \left( \frac{\partial^2 f}{\partial \rho_1^2} \right) \rho_1^2 + \frac{1}{2} \left( \frac{\partial^2 f}{\partial \rho_2^2} \right) \rho_2^2 \\ & + \frac{1}{2} \left( \frac{\partial^3 f}{\partial \rho_1^2 \partial \rho_2} \right) \rho_1^2 \rho_2 + \frac{1}{4!} \left( \frac{\partial^4 f}{\partial \rho_1^4} \right) \rho_1^4 \\ & + \frac{1}{4!} \left( \frac{\partial^4 f}{\partial \rho_2^4} \right) \rho_2^4 + \frac{1}{4} \left( \frac{\partial^4 f}{\partial \rho_1^2 \partial \rho_2^2} \right) \rho_1^2 \rho_2^2, \end{aligned} \quad (17)$$

where  $f_0$  is the free energy of the nematic phase and the derivatives have been evaluated at  $\rho_1 = \rho_2 = 0$ . The above expansion includes all terms (up to the fourth order) compatible with the requirement that the free energy be independent of an arbitrary uniform translation of  $\rho(z)$  [54]. At fixed average density and temperature, the free energy must be a minimum with respect to variations in the order parameters. Solving the stationary condition  $(\partial f / \partial \rho_2) = 0$  allows expressing  $\rho_2$  in terms of the leading order parameter  $\rho_1$ . Considering that  $\rho_1$  is small in the neighborhood of the transition,  $\rho_2$  is given, to lowest order in  $\rho_1$ , by

$$\rho_2 = \frac{-(\partial^3 f / \partial \rho_1^2 \partial \rho_2)}{2(\partial^2 f / \partial \rho_2^2)} \rho_1^2. \quad (18)$$

Substituting  $\rho_2$  from (18) into the expansion of the free energy given in Eq. (17), one obtains up to fourth order in  $\rho_1$ :

$$f(T, \rho; q, \rho_n) = f_0(T, \rho) + \frac{1}{2} a_2 \rho_1^2 + \frac{1}{4!} a_4 \rho_1^4 + \dots \quad (19)$$

The line of bifurcation points follows from the conditions [20]

$$a_2(T, \rho^*; q^*) \equiv \frac{\partial^2 f}{\partial \rho_1^2} = 0, \quad \frac{\partial a_2}{\partial q}(T, \rho^*; q^*) = 0, \quad (20)$$

where  $d^* = 2\pi/q^*$  is the layer spacing at the bifurcation point. Determination of the order of the transition requires calculating the coefficient  $a_4$  in the expansion (19). This coefficient is given by

$$a_4(T, \rho; q) = \left( \frac{\partial^4 f}{\partial \rho_1^4} \right) - 3 \left( \frac{\partial^3 f}{\partial \rho_2 \partial \rho_1^2} \right) \left/ \left( \frac{\partial^2 f}{\partial \rho_2^2} \right) \right. \quad (21)$$

Typically, the condition  $a_4(T, \rho; q) = 0$ , along with (20), fixes the location of the tricritical point, provided the next-order coefficient ( $a_6$ ) in the expansion (19) be positive [54,55]. If this is the case, then the transition is continuous for  $a_4 > 0$  and first order for  $a_4 < 0$ . However, we have found conditions at which the transition was clearly first order even though  $a_4 > 0$ . We have noticed that a similar claim has been given by Poniewerski and Sluckin [30]. Our procedure to locate the tricritical point is similar to that used by Poniewerski and Sluckin [30], and is based upon the analysis of the equation of state  $P = P(\rho, T)$ , where  $P$  is the pressure, in the neighborhood of the bifurcation point. Consider a temperature  $T$  at which the nematic–smectic- $A$  transition is continuous. In this case, the slope of the equation of state on the high-density (smectic) side of the transition must be positive (as a result of the condition of mechanical stability) in any arbitrarily small neighborhood of the bifurcation point. On the other hand, if the transition happens to be first order, the smectic equation of state branches off from the bifurcation point with a negative slope. It can be shown that the slope of the smectic branch of the equation of state at the bifurcation point can be written as

$$\left( \frac{\partial P}{\partial \rho} \right)_A^* = \left( \frac{\partial P}{\partial \rho} \right)_N^* - 3\rho^* \frac{(\partial a_2 / \partial \rho)^*}{a_4^*}, \quad (22)$$

where the subscripts  $A$  and  $N$  refer to the smectic- $A$  and nematic phase, respectively, and the asterisk indicates evaluation at the bifurcation point. The tricritical point then follows from the condition

$$\left( \frac{\partial P}{\partial \rho} \right)_A^* = 0, \quad (23)$$

along with (20). Poniewerski and Sluckin [30] give a similar condition but involving the isothermal compressibility  $\kappa_T$ . Both expressions are obviously related after noticing that  $\kappa_T^{-1} = \rho(\partial P / \partial \rho)$ . [Note that Eq. (22) reduces to Eq. 4.4 in Ref. [30] except for an extra density factor appearing in the latter

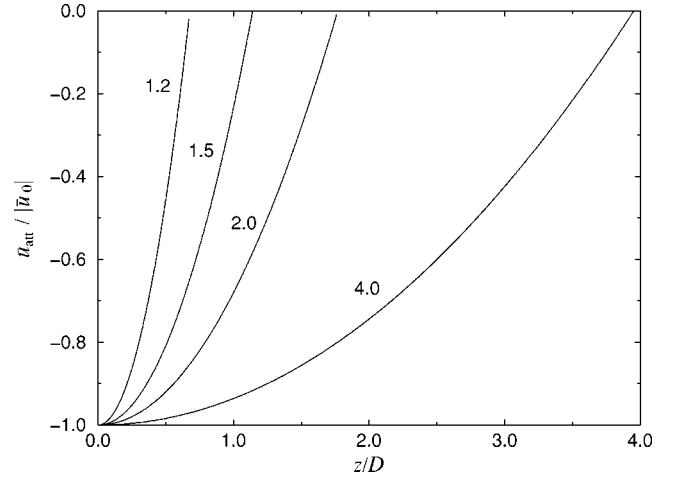


FIG. 1. Effective attractive pair potential  $\bar{u}_{\text{att}}$  as a function of the intermolecular distance  $z/D$  for different values of the range of the attractive interactions  $\lambda/D$  (labeled on the plot). The effective potential is normalized by  $|u_0|$  defined by Eq. (14).

equation, probably due to a typographical error. It is straightforward to check that Eq. (22) is dimensionally correct.]

#### IV. RESULTS

For given input values of the average density  $\rho$  and temperature  $T$ , the free energy (15) was minimized with respect to the wavevector  $q$  and the set of translational parameters  $\rho_n$  with  $n = 1, \dots, m$ . In our calculations we used  $m = 10$  in the Fourier expansion of the density distribution  $\rho(z)$  in Eq. (16). Once the set of variational parameters that minimizes  $f$  is found, the pressure ( $P$ ) and chemical potential can be readily calculated from the free energy. The homogeneous nematic phase is characterized by  $q = 0$  and  $\rho_n = 0$ . In this case, both  $\rho(z)$  and  $\bar{\rho}(z)$  reduces to the average number density  $\rho$ . In all calculations reported here, the molecular elongation was given a value  $L/D = 5$ . The temperature will be always reported in units of  $\epsilon/k_B$ .

As a check of the consistency of our approach, we first considered the case  $\lambda/D = 1$ . For this choice,  $z_{\text{max}}$  [see Eq. (13)] turns out to be zero. Therefore, the effective attractive interaction vanishes and the free energy in Eq. (15) contains only the contributions from the hard cores. In this case, Eq. (20) was found to have no solution at typical fluid densities. Hence, smectic ordering is not promoted in this model in the absence of attractions [11]. This is consistent with the fact that, under these circumstances, no smectic phase is to be expected [52].

The effective attractive potential is shown in Fig. 1 for a few values of the range parameter  $\lambda$ . Figure 1 illustrates how averaging the spherically symmetric square-well interactions outside the ellipsoidal core gives rise to an anisotropy in the attractive potential. According to Fig. 1, the main effect is to emphasize the attractions in the equatorial region ( $z = 0$ ). As a result, this is expected to stabilize configurations in which molecular pairs are side by side. Although the attractive interactions seem to promote a layered configuration, the latter

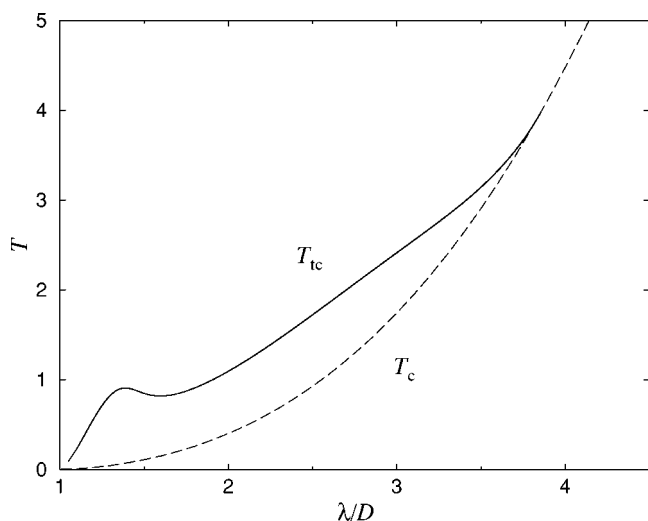


FIG. 2. Nematic-nematic critical temperature  $T_c$  (dashed curve) and tricritical temperature  $T_{tc}$  (continuous curve) for a system of parallel hard ellipsoids of anisotropy  $L/D=5$  as a function of the range  $\lambda/D$  of the attractive well. The temperature is given in units of  $\epsilon/k_B$ .

may correspond to a smectic or a solid structure.

The model fluid was found to exhibit phase separation at temperatures below a critical temperature  $T_c$  when attractive interactions are explicitly included ( $\lambda/D > 1$ ). This is the equivalent of the usual vapor-liquid equilibria, although in the present case (where the isotropic phase is ruled out) the phase equilibria involves a low-density and a high-density nematic phase. Increasing the value of  $\lambda$  has the trivial effect of promoting the nematic-nematic separation to higher temperatures. The dependence of  $T_c$  upon variations in  $\lambda$  is depicted in Fig. 2.

Next we proceeded to investigate whether smectic ordering is promoted by attractive interactions with  $\lambda/D > 1$ . At any given temperature, Eq. (20) may be solved for the density at the bifurcation point. It was found that for any arbitrarily small value of  $\lambda$  the nematic phase is destabilized at some density, favoring the onset of smecticlike fluctuations. The limit of stability of the nematic phase with respect to a smectic density modulation is plotted in Figs. 3 and 4 in the pressure-temperature and temperature-density plane, respectively, for several values of the range parameter between  $1.0 < \lambda/D < 2.0$ . In Fig. 3, the smectic-A phase corresponds, for each value of  $\lambda$ , to the low-temperature, high-pressure region. In Fig. 4, the Sm-A phase occupies the high-density region. As stated in Sec. III, our approach does not give account of the solid phase and, consequently, yields no information on the stability of the smectic phase relative to the solid phase. Nonetheless, a useful guide is provided by the fluid ( $F$ )-to-solid ( $S$ ) transition in a system of hard spheres. Recall that in the absence of attractive interactions, the properties of our system can be exactly related to those of a system of hard spheres under appropriate anisotropic scaling. Using the values of the  $F$ - $S$  transition for hard spheres from Hoover and Ree [56], the solid phase is thermodynamically stable at pressures above  $(P_{V_0}/k_B T)_{FS} = 6.12$ . The densities of the coexisting fluid and solid phases are [56]  $\eta_F = 0.494$  and

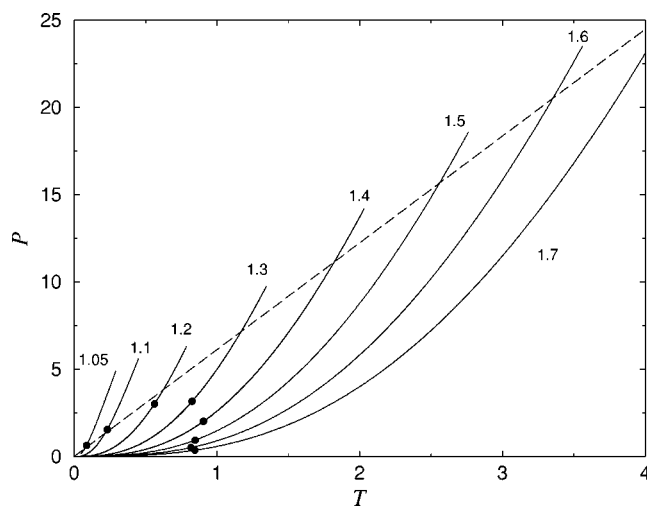


FIG. 3. Bifurcation curves showing the limit of stability of the nematic phase with respect to a smectic density modulation for a system of parallel hard ellipsoids of anisotropy  $L/D=5$  and different values of the range  $\lambda/D$  of the attractive well (labeled on the plot) in the pressure-temperature ( $P$ - $T$ ) plane. The smectic phase corresponds in each case to the low-temperature, high-pressure region. The filled circles indicate the location of the tricritical point for each value of  $\lambda$ . The dashed curve represents the fluid-solid boundary line for the case  $\lambda/D=1$ . The temperature is given in units of  $\epsilon/k_B$  and the pressure is in units of  $\epsilon/v_0$ , with  $v_0$  being the molecular volume.

$\eta_S = 0.545$ , respectively. These values would apply here for the case  $\lambda/D=1$ . The melting line and fluid-solid coexistence region for  $\lambda/D=1$  have been included in Figs. 3 and 4. Explicit consideration of the attractive interactions ( $\lambda/D > 1$ ) will be expected to give rise to a shift of the melting line to lower pressures (or higher temperatures) and to a shift of the fluid-solid coexistence region to lower densities. These shifts are expected to be quantitatively important at low temperature, but progressively small with increasing temperature

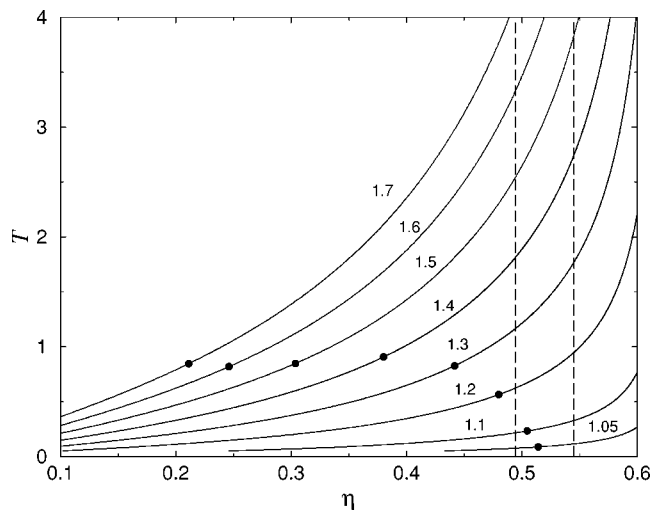


FIG. 4. As in Fig. 3 but shown in the temperature-density ( $T$ - $\eta$ ) plane. The smectic phase corresponds for each value of  $\lambda/D$  to the high-density region.  $\eta$  is the packing fraction.

when attractions turn negligible. It follows that the fluid-to-solid transition lines for  $\lambda/D=1$  provide upper limits for the stability of the fluid phase relative to the solid when  $\lambda/D > 1$ .

For the smallest values of  $\lambda$ , stabilization of the smectic phase was seen to occur either at very low temperatures (where our perturbativelike approach is not expected to be very reliable) or at densities at which the formation of the solid phase is more likely to occur. Therefore, we claim that very short range attractive interactions will not give rise to smectic ordering. From Figs. 3 and 4 we tentatively estimate the above conclusion to hold for  $1.0 < \lambda/D < 1.3$ . Above  $\lambda/D \approx 1.3$ , the smectic phase becomes stable at densities (and temperatures) well before crystallization might take place. According to Figs. 3 and 4, the bifurcation lines move to higher temperatures and lower densities with increasing  $\lambda$ . Thus increasing the range of the attractive interactions has the effect of increasing the range of stability of the smectic phase relative to the nematic phase. Interestingly, this effect is seen to be reversed at some intermediate value ( $\lambda/D \approx 2.5$ ). For higher values, the region over which the nematic phase is stable becomes wider. For larger values of the range parameter ( $\lambda/D=4.1$ ) the bifurcation equation was found to have no physical solution at any thermodynamic condition. Thus we conclude that smectic ordering is no longer promoted when the attractive interactions are made too long ranged.

We next considered the case  $\lambda/D=1.5$  and concentrated on the behavior of the system in the supercritical region. The nematic-nematic critical point was found at a value of  $T_c = 0.108$ . The loci of the bifurcation densities is shown in the pressure-density plane in Fig. 5. We also include in the figure the equation of state  $P=P(\eta, T)$  for selected temperatures. In all cases, the low-density branch of the isotherms corresponds to the nematic phase. At each temperature, the nematic phase is expected to be unstable against smectic fluctuations at the corresponding bifurcation packing fraction  $\eta^*$ . This is compatible with the observed change in slope of the equations of state at  $\eta^*$ . According to Fig. 5, the smectic phase branches off from the bifurcation point with a positive slope at high temperatures. This corresponds to a continuous nematic-smectic-A transition. At lower temperatures, on the other hand, the slope of the smectic branch was found to be negative (mechanically unstable) in some neighborhood of the bifurcation point and positive (mechanically stable) at slightly higher densities. This indicates that the nematic phase undergoes a first-order transition to the smectic phase at these temperatures. The tricritical point separating these two regimes was calculated according to Eq. (23). The variation of the tricritical temperature  $T_{tc}$  with  $\lambda$  has been included in Fig. 2. According to the figure,  $T_{tc}$  exhibits a non-trivial pattern at low values of  $\lambda$  followed by a steady increase as the attractions are made longer ranged. No tricritical point was found for values  $\lambda/D \geq 3.85$ .

The phase diagram for the case  $\lambda/D=1.5$  is shown in Fig. 6 in the temperature-density plane. The tricritical point is located at  $T_{tc}=0.847$ , with  $\eta_{tc}=0.304$ , and  $(Pv_0/\epsilon)_{tc}=0.937$ . For temperatures  $T > T_{tc}$ , the nematic-smectic-A transition is continuous and the coexistence line is given by the bifurca-

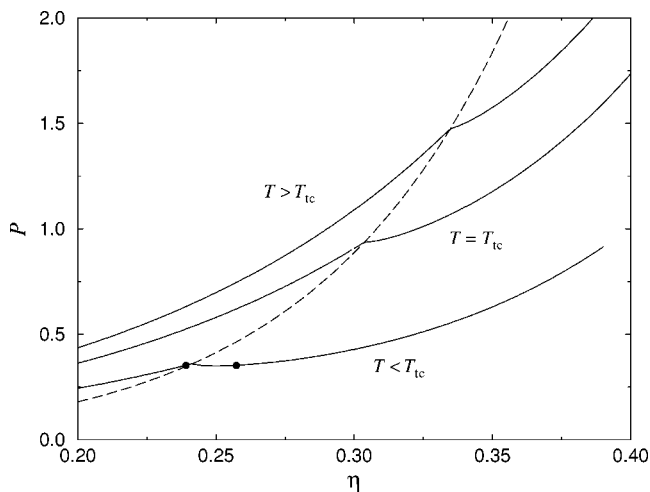


FIG. 5. Equation of state in the pressure-density ( $P$ - $\eta$ ) plane for a system of parallel hard ellipsoids of anisotropy  $L/D=5$  with  $\lambda/D=1.5$  for various temperatures  $T$ . From top to bottom the values of the temperature are  $T=1.0, 0.847, \text{ and } 0.6$  in units of  $\epsilon/k_B$ . The tricritical temperature is  $T_{tc}=0.847$ . The dashed curve represents the line of bifurcation densities. The smectic-A phase corresponds to the high-density region. The closed circles show the location of the first-order nematic-smectic-A transition at  $T=0.6$ . The pressure is given in units of  $\epsilon/v_0$ , with  $v_0$  being the molecular volume.  $\eta$  is the packing fraction.

tion line. For temperatures  $T < T_{tc}$ , the transition is first order and the corresponding transition densities were calculated by equating the pressure and chemical potential in both phases. As can be observed in Fig. 6, the nematic-smectic-A transition takes place at increasingly higher densities as the temperature increases. From our previous remarks, the nematic-

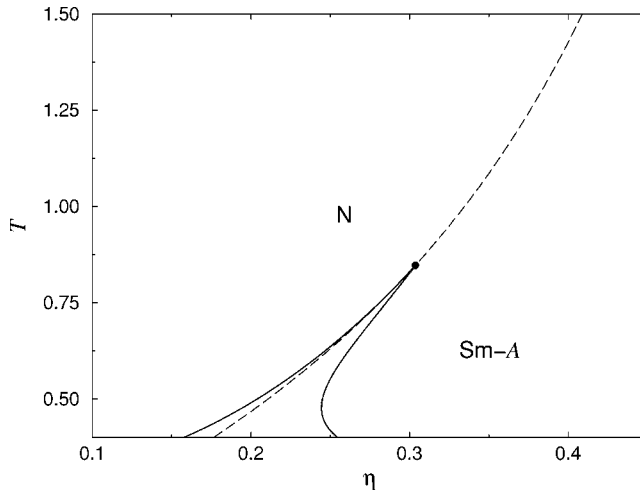


FIG. 6. Phase diagram for a system of hard ellipsoids of anisotropy  $L/D=5$  and attractive range  $\lambda/D=1.5$  in the temperature-density ( $T$ - $\eta$ ) plane showing the regions of stability of the nematic (N) and smectic-A (Sm-A) phases. The dashed curve represents the line of bifurcation points. Above the tricritical point (filled circle), the N-Sm-A transition is continuous. The solid curves correspond to first-order N-Sm-A transitions. Nematic-nematic separation takes place for  $T < 0.108$  and is not visible in the scale of the plot. The temperature is given in units of  $\epsilon/k_B$ , and  $\eta$  is the packing fraction.

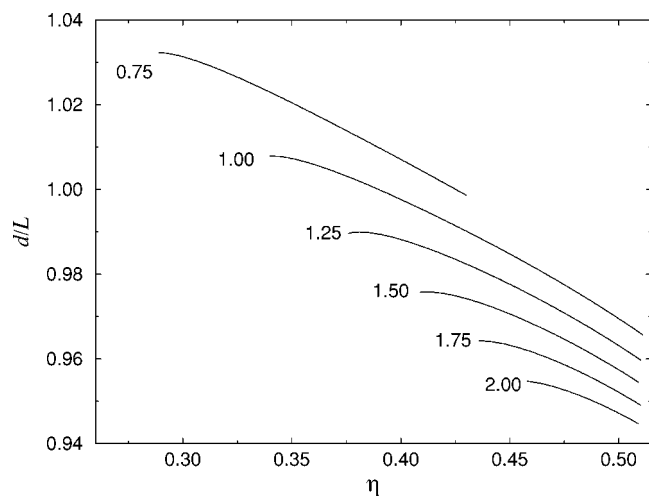


FIG. 7. Variation of the smectic spacing  $d/L$  with packing fraction  $\eta$  at different values of the temperature  $T$  (labeled on the plot) for a system of parallel hard ellipsoids of anisotropy  $L/D=5$ . The range of the attractive interactions is  $\lambda/D=1.5$ .

smectic- $A$  transition is expected to be preempted by the formation of the solid phase at sufficiently high temperature.

We show in Fig. 7 the variation of the smectic layer spacing  $d$  with density along a number of selected isotherms when  $\lambda/D=1.5$ . In all cases,  $d$  is seen to decrease smoothly with increasing density or temperature. The value of  $d$  was always found to be of the order of the molecular length  $L$ .

We emphasize again that our approach is able to describe the stability of the smectic phase relative to the nematic but yields no information as regards the relative stability with respect to the solid phase. Bearing this in mind, one may still wonder whether or not the solid phase preempts the formation of the smectic phase, thereby leaving the latter merely as metastable. A fully consistent theoretical description of the solid phase involves considerable numerical complication and it was not considered here. Instead, the relative stability of the solid and smectic phases was assessed by using computer simulation.

Simulation results are given in Fig. 8 for the model used here with molecular anisotropy  $L/D=5$  and attractive range  $\lambda/D=1.5$ . Most simulations were performed in the  $NPT$  ensemble using standard Monte Carlo techniques. Details will be given elsewhere [57]. Figure 8 includes part of the results obtained by expanding a solid configuration at high densities and pressures (higher than those shown in the figure) along two constant-temperature paths. At  $T=1.0$ , the solid is seen to melt into a smectic- $A$  phase at  $Pv_0/\epsilon \approx 1.45$  with  $\eta_A \approx 0.39$  and  $\eta_S \approx 0.43$ . When compressing the system from low densities, the smectic- $A$  phase was seen to crystallize at a slightly larger pressure ( $Pv_0/\epsilon \approx 2.0$ ). As expected, the smectic-solid transition is first order and exhibits hysteresis. Therefore, the quoted values of the pressure represent the limits of mechanical stability of the solid and smectic phases upon expansion and compression of the system. The transition pressure, as well as the densities of the coexisting phases, will be somewhere in between. The smectic phase was also seen to be stable relative to the solid at  $T=0.6$ . Simulation results along this isotherm are shown in Fig. 8. At

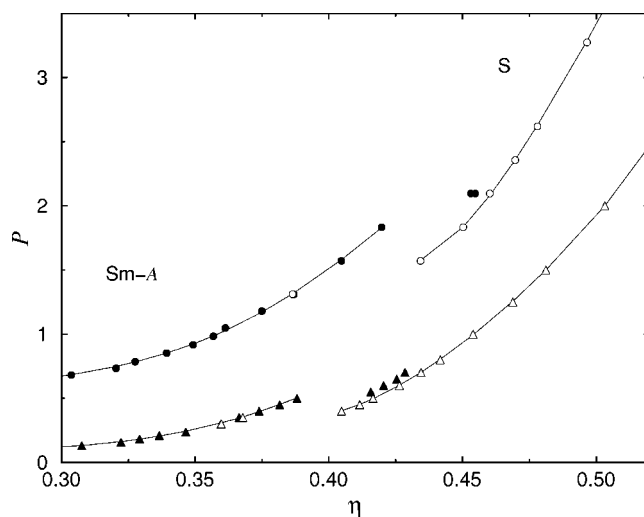


FIG. 8. Detail of the smectic- $A$ -solid (Sm- $A$ -S) transition region for a system of hard ellipsoids of anisotropy  $L/D=5$  and attractive range  $\lambda/D=1.5$ . Data have been obtained from Monte Carlo simulations in the  $NPT$  ensemble along two isotherms  $T=1.0$  (circles) and  $T=0.6$  (triangles). The open symbols are for results obtained expanding a solid configuration. The closed symbols are for results obtained after compressing from a fluid configuration. The curves are included as a guide to the eye. The temperature is in units of  $\epsilon/k_B$ , the pressure is in units of  $\epsilon/v_0$ , and  $\eta$  is the packing fraction.

this temperature, the smectic-solid transition takes place at slightly lower densities and pressure, as expected. When the system is expanded to densities below those shown in Fig. 8, the smectic phase undergoes a transition to a nematic fluid. The results from simulation in this region are shown in Fig. 9. At  $T=1.0$  the nematic-smectic- $A$  transition seems to proceed in a continuous way at a density  $\eta_{NA} \approx 0.27$ , the value of the pressure being  $Pv_0/\epsilon \approx 0.60$ . The theoretical calculations yield a continuous transition at this temperature with  $\eta_{NA}=0.335$ ,  $Pv_0/\epsilon=1.47$ . At temperature  $T=0.6$  the nematic-smectic- $A$  transition was observed to be clearly first order. As shown in Fig. 9, results from  $NVT$  Monte Carlo simulations give evidence of a van der Waals-like loop at this temperature (these simulations were performed at constant volume but allowing for changes in the box shape). From the simulation results we can infer that the transition takes place at  $Pv_0/\epsilon \approx 0.088$ , the transition densities being  $\eta_N \approx 0.18$  and  $\eta_A \approx 0.25$ . The theory (see Fig. 6) predicts a first-order nematic-smectic- $A$  transition at this temperature with  $\eta_N=0.239$ ,  $\eta_A=0.257$ , and  $Pv_0/\epsilon=0.135$ .

As noted before, the region of stability of the smectic- $A$  phase must be bounded at high temperature (and pressure). Several exploratory runs were performed by expanding a solid configuration along different constant-temperature paths. For  $\lambda/D=1.5$ , our results indicated that the solid phase melts directly into the nematic phase with no intermediate smectic phase for temperatures above  $T \approx 3.25$  [57].

From the simulation results we infer that there are thermodynamic conditions at which the smectic phase is stable not only relative to the nematic phase, but also relative to the solid phase. Although the simulations have been restricted to



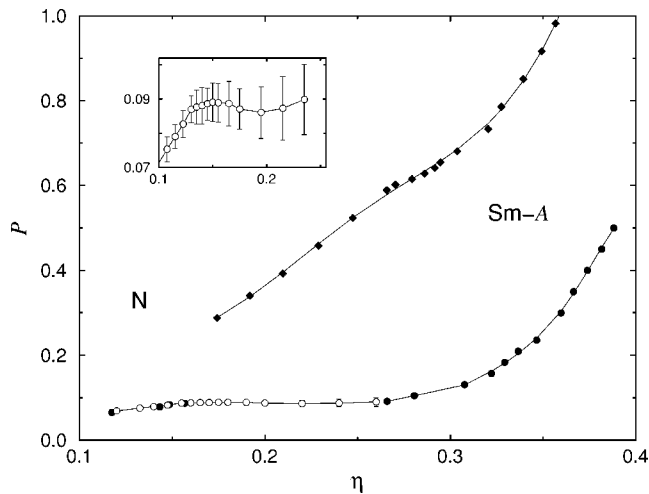


FIG. 9. Nematic–smectic-A (N–Sm-A) transition region for a system of hard ellipsoids of anisotropy  $L/D=5$  and attractive range  $\lambda/D=1.5$  at temperatures  $T=1.0$  (diamonds) and  $T=0.6$  (circles) as obtained from Monte Carlo simulations at constant pressure (filled symbols) and constant volume (open symbols). The inset shows the first-order N–Sm-A transition at temperature  $T=0.6$  on a magnified scale. The curves are included as a guide to the eye. The temperature is in units of  $\epsilon/k_B$ , the pressure is in units of  $\epsilon/v_0$ , and  $\eta$  is the packing fraction.

a single value of  $\lambda$ , the conclusions are expected to be appropriate for other values of  $\lambda$ . The simulation data are also consistent with the prediction of a temperature-induced tricritical point, and the disappearance of the smectic phase at high temperatures. The agreement between theoretical predictions and simulation results can be considered satisfactory at a qualitative level. Not surprisingly, there are quantitative discrepancies. This can certainly be ascribed to the use of the mean-field approximation, which is known to underestimate the contributions from molecular correlations at short distances.

## V. SUMMARY AND CONCLUSIONS

The motivation of this work is to gain an understanding of the behavior of thermotropic smectic liquid crystals. A number of molecular theories neglect the effect of hard cores and point at the anisotropic attractive interactions as responsible for smectic ordering in thermotropics, whereas simulations (as well as microscopic theories) of systems of hard particles have stressed the importance of the anisotropic excluded-volume interactions in driving smectic formation. Here we have focused on two specific points; first, whether smectic ordering may be brought about by the coupling between the anisotropic short-range repulsions and the isotropic contribution of the soft, long-range attractions; and second, what is the role (if any) of the range of the soft attractions in stabilizing the smectic phase. In our approach this requires a suitable molecular model and an appropriate theory for describing the inhomogeneous smectic phase.

As regards the molecular model, we have considered a system of hard ellipsoids to mimic excluded volume effects

with an attractive square well of range  $\lambda/D > 1$  with spherical symmetry outside the hard core. In a way, the model can be considered as the natural extension of the square-well model for simple fluids to systems of nonspherical particles. The model is certainly a crude representation of the molecular interactions, but still contains the simplest microscopic features which are thought to be responsible for stabilizing the smectic phase in thermotropic liquid crystals.

As regards the theoretical approach, we have used a density-functional theory based upon an extension of the weighted-density approximation to systems with anisotropic interactions. This is known to provide a fairly accurate and consistent description of the contributions arising from the hard cores. The attractive contributions are treated at a mean-field level. The shortcomings of mean-field treatments are well known, and obviously our approach suffers from the same limitations. The theory has been applied to systems of perfectly aligned molecules, although it can also be extended to the general case where molecules are free to rotate. The region in which the smectic phase turns out to be stable relative to the nematic has been investigated using a bifurcation analysis, and a full phase stability calculation.

From our calculations, the effects on phase behavior due to variations on  $\lambda$  are as follows. For very small values of  $\lambda$  (approximately,  $\lambda/D < 1.3$ ) thermodynamic conditions are found at which nematic order becomes unstable against a smectic modulation. However, these conditions are such that the solid phase is more likely to dominate. For this range of values of  $\lambda$ , the attractions are very short ranged and the effective attractions are not sufficiently anisotropic to bring about smectic ordering. The phase behavior corresponds, essentially, to that expected for a system of parallel hard ellipsoids, i.e., nematic phase and a solid phase at high density. Upon increasing  $\lambda$ , the induced anisotropy is large enough so as to stabilize smectic ordering. At very low temperatures, the smectic phase is again expected to be metastable relative to the solid, but at intermediate temperatures it is certainly stable at densities well before crystallization, as demonstrated by computer simulation. The nematic–smectic-A transition is seen to be continuous at high temperature and first order at low temperature, both regimes being separated by a tricritical point. By construction, our approach does not allow for a description of the solid phase. The stability of the smectic phase relative to the solid phase has nonetheless been proved by computer simulation. Although no calculation of the smectic–solid phase boundaries can be performed within our theoretical treatment, some hint is given from knowledge of the fluid–solid phase boundaries of the model with  $\lambda/D=1$ . Note that the latter provide an upper limit for the smectic- (or nematic-) solid phase boundaries when  $\lambda/D > 1$ . Interestingly, our calculations show that the nematic–smectic-A bifurcation line must intersect the fluid–solid line at sufficiently high temperatures. It follows that the smectic phase in the present model does not extend to arbitrarily high pressures or temperatures. This has been confirmed by our computer simulation results. A similar conclusion holds for the Gay-Berne model [58,59], and is consistent with the fact that under these conditions the attractive interactions become less important and the hard ellipsoidal cores are not able to stabilize smectic ordering. We recall

that it is not infrequent to observe a decrease in the range of the smectic phase under the application of hydrostatic pressure, or the suppression of the smectic phase beyond a certain value of the pressure [60].

Upon further increase of  $\lambda$ , the system stabilizes smectic ordering at increasingly higher temperatures. The anisotropic interactions are such that the typical side-by-side molecular configurations of the smectic phase are largely promoted. When  $\lambda$  is further increased, the minimum of the effective interactions about  $z=0$  (see Fig. 1) becomes increasingly wider. Hence, the number of molecular configurations other than the side-by-side which are energetically equivalent increases and this results in a growing tendency to destabilize the smectic layering. According to our calculations, the nematic phase completely dominates the fluid region of the phase diagram at  $\lambda/D \approx 4.0$ .

It would be desirable to provide a more complete computer simulation study of the model in order to establish the merits and limitations of the theoretical approach on a firmer footing. Work along this avenue is in progress and will be presented elsewhere [57]. The numerical techniques used

here can be extended to accommodate hard disk-shaped ellipsoids. In such a case, the anisotropic interactions are expected to stabilize the columnar phase between the solid and nematic phases [61]. Finally, we are also considering a more general treatment in which the constraint of perfect alignment is removed. We hope to present the results of this investigation in a future publication.

#### ACKNOWLEDGMENTS

We are thankful to G. Jackson and A. Galindo for fruitful discussions and express our gratitude for their hospitality during a sabbatical at Imperial College London. This work was made possible by financial support from the Dirección General de Investigación (Spain) under Project No. FIS2004-06227-C02-01, Junta de Andalucía, and Plan Propio de la Universidad de Huelva. E. de M. also acknowledges financial support from Secretaría de Estado de Educación y Universidades (Spain) within the Programa de Movilidad de Profesorado.

- 
- [1] S. Singh, *Phys. Rep.* **324**, 107 (2000).  
 [2] M. A. Osipov, in *Handbook of Liquid Crystals*, edited by D. Demus, J. W. Goodby, C. W. Gray, H.-W. Spiess, and V. Vill (Wiley-VCH, Weinheim, 1998), Vol. 1, Chap. 2.  
 [3] J. P. Hansen and I. R. MacDonald, *Theory of Simple Liquids* (Academic Press, London, 1986).  
 [4] S. Chandrasekhar, *Liquid Crystals*, 2nd ed. (Cambridge University Press, Cambridge, England, 1992).  
 [5] W. L. McMillan, *Phys. Rev. A* **4**, 1238 (1971); *Phys. Rev. A* **6**, 936 (1972).  
 [6] K. K. Kobayashi, *J. Phys. Soc. Jpn.* **29**, 101 (1970).  
 [7] F. T. Lee, H. T. Tan, Y. M. Shih, and C.-W. Woo, *Phys. Rev. Lett.* **31**, 1117 (1973).  
 [8] P. J. Photinos and A. Saupe, *Phys. Rev. A* **13**, 1926 (1976).  
 [9] L. Senbetu and C.-W. Woo, *Phys. Rev. A* **17**, 1529 (1978).  
 [10] G. R. Kventsel, G. F. Luckhurst, and H. B. Zewdie, *Mol. Phys.* **56**, 589 (1985).  
 [11] L. Mederos and D. E. Sullivan, *Phys. Rev. A* **39**, 854 (1989).  
 [12] Even if the soft attractive interactions were the dominant effect in stabilizing smectic order, a quantitative description would only be possible with an accurate description of the short-range repulsive interactions.  
 [13] L. Onsager, *Ann. N.Y. Acad. Sci.* **51**, 627 (1949).  
 [14] A. Stroobants, H. N. W. Lekkerkerker, and D. Frenkel, *Phys. Rev. Lett.* **57**, 1452 (1986).  
 [15] A. Stroobants, H. N. W. Lekkerkerker, and D. Frenkel, *Phys. Rev. A* **36**, 2929 (1987).  
 [16] S. C. McGrother, D. C. Williamson, and G. Jackson, *J. Chem. Phys.* **104**, 6755 (1996).  
 [17] P. Bolhuis and D. Frenkel, *J. Chem. Phys.* **106**, 666 (1997).  
 [18] For an excellent review, see M. P. Allen, G. T. Evans, D. Frenkel, and B. M. Mulder, *Adv. Chem. Phys.* **86**, 1 (1993).  
 [19] G. Vertogen and W. H. de Jeu, *Thermotropic Liquid Crystals: Fundamentals*, Springer Series in Chemical Physics Vol. 95 (Springer-Verlag, Berlin, 1988).  
 [20] B. Mulder, *Phys. Rev. A* **35**, 3095 (1987).  
 [21] B. Tjijto-Margo and G. T. Evans, *J. Chem. Phys.* **93**, 4254 (1990).  
 [22] P. Tarazona, *Philos. Trans. R. Soc. London, Ser. A* **344**, 307 (1993).  
 [23] A. M. Somoza and P. Tarazona, *Phys. Rev. Lett.* **61**, 2566 (1988).  
 [24] A. M. Somoza and P. Tarazona, *J. Chem. Phys.* **91**, 517 (1989).  
 [25] A. M. Somoza and P. Tarazona, *Phys. Rev. A* **41**, 965 (1990).  
 [26] E. Velasco, L. Mederos, and T. J. Sluckin, *Liq. Cryst.* **20**, 399 (1996).  
 [27] E. Velasco, L. Mederos, and D. E. Sullivan, *Phys. Rev. E* **62**, 3708 (2000).  
 [28] A. Poniewierski and R. Holyst, *Phys. Rev. Lett.* **61**, 2461 (1988).  
 [29] R. Holyst and A. Poniewierski, *Phys. Rev. A* **39**, 2742 (1989).  
 [30] A. Poniewierski and T. J. Sluckin, *Phys. Rev. A* **43**, 6837 (1991).  
 [31] H. Graf and H. Löwen, *J. Phys.: Condens. Matter* **11**, 1435 (1999).  
 [32] P. Tarazona, *Phys. Rev. A* **31**, 2672 (1985).  
 [33] W. M. Gelbart and B. A. Baron, *J. Chem. Phys.* **66**, 207 (1977).  
 [34] W. M. Gelbart and A. Gelbart, *Mol. Phys.* **33**, 1387 (1977).  
 [35] M. A. Cotter, *J. Chem. Phys.* **66**, 4710 (1977).  
 [36] B. A. Baron and W. M. Gelbart, *J. Chem. Phys.* **67**, 5795 (1977).  
 [37] M. A. Cotter, in *The Molecular Physics of Liquid Crystals*, edited by G. R. Luckhurst and C. W. Gray (Academic Press, London, 1979).  
 [38] B. Barbooy and W. M. Gelbart, *J. Chem. Phys.* **71**, 3053 (1979).

- [39] W. M. Gelbart, J. Phys. Chem. **86**, 4298 (1982).
- [40] A. Kloczkowski and J. Stecki, Mol. Phys. **55**, 689 (1985).
- [41] M. Nakagawa and T. Akahane, J. Phys. Soc. Jpn. **53**, 1951 (1984).
- [42] D. R. Evans, G. T. Evans, and D. K. Hoffman, J. Chem. Phys. **93**, 8816 (1991); G. T. Evans and E. B. Smith, Mol. Phys. **74**, 79 (1991).
- [43] B. Tjipto-Margo and G. T. Evans, Mol. Phys. **74**, 85 (1991).
- [44] E. de Miguel and M. P. Allen, Mol. Phys. **76**, 1275 (1992).
- [45] D. C. Williamson, Mol. Phys. **95**, 319 (1998).
- [46] S. Varga and I. Szalai, Mol. Phys. **95**, 515 (1998).
- [47] S. Varga, D. C. Williamson, and I. Szalai, Mol. Phys. **96**, 1695 (1999).
- [48] P. I. C. Texeira, Mol. Phys. **92**, 167 (1997).
- [49] D. C. Williamson and F. del Río, J. Chem. Phys. **109**, 4675 (1998).
- [50] D. C. Williamson and Y. Guevara, J. Phys. Chem. B **103**, 7522 (1999).
- [51] E. García, D. C. Williamson, and A. Martínez-Richa, Mol. Phys. **98**, 179 (2000).
- [52] P. Harrowell and D. W. Oxtoby, Mol. Phys. **54**, 1325 (1985).
- [53] W. H. Press, S. A. Teukolsky, W. T. Vetterling, and B. P. Flannery, *Numerical Recipes* (Cambridge University Press, Cambridge, England, 1986).
- [54] R. B. Meyer and T. C. Lubensky, Phys. Rev. A **14**, 2307 (1976).
- [55] L. Longa, J. Chem. Phys. **85**, 2974 (1985).
- [56] W. G. Hoover and F. H. Ree, J. Chem. Phys. **49**, 3609 (1968).
- [57] E. de Miguel and E. Martín del Río (unpublished).
- [58] J. T. Brown, M. P. Allen, E. Martín del Río, and E. de Miguel, Phys. Rev. E **57**, 6685 (1998).
- [59] E. de Miguel, E. Martín del Río, and F. J. Blas, J. Chem. Phys. **121**, 11183 (2004).
- [60] P. Pollmann, in *Physical Properties of Liquid Crystals*, edited by D. Demus, J. Goodby, G. W. Gray, H.-W. Spiess, and V. Vill (Wiley-VCH, Weinheim, 1999), p. 253.
- [61] E. Martín del Río, A. Galindo, and E. de Miguel (unpublished).